Copyright © 1998, by the International Council of the Aeronautical Sciences (ICAS)
and the American Institute of Aeronautics and Astronautics, Inc.

A98-31570 ICAS-98-3,10,4

PLIF IMAGING OF THE SEPARATED REGION BEHIND A CONE IN A HYPERSONIC FLOW

S. O'Byrne, P.C. Palma, P.M. Danehy, N.R. Mudford* , S.L. Gai * and A.F.P. Houwing

Australian National University, Canberra, ACT, Australia

*School of Aerospace and Mechanical Engineering, Australian Defence Force Academy, Canberra, ACT, Australia

Abstract

Experiments have been performed which examine the development of separated flow in the near-wake of a cone in a hypersonic freestream. Planar laser-induced fluorescence (PLIF) has been successfully used to visualise the flow around the base of the cone in a Mach 7.6 freestream at various times after the onset of flow. The images show the time-evolution of the main features of the separated flow. They also demonstrate that the shock tunnel flow time is sufficiently long-lived to establish a steady flow in the shock layer. There is, however, evidence to suggest that the flow in the separated region did not reach a steady state during the 400 microseconds after shock reflection. Calculations based upon previous pressure data for base flows behind spheres appear to underestimate the establishment time for the separated flow behind the cone.

1. Introduction

The free-piston shock tunnel is a useful tool for the study of hypersonic flow phenomena. This ground-based flow facility offers a less expensive and more easily controlled means of testing than in-flight measurements. Free-piston shock tunnels have been used extensively in the past to examine many types of supersonic and hypersonic flows[1] which, due to their high speeds and stagnation temperatures, cannot be examined in longer-duration wind tunnel facilities.

Despite the fact that shock tunnels can be used to generate both non-reacting and reacting hypersonic flows, one major difficulty associated with using these facilities is their extremely short flow duration. This problem becomes particularly serious when examining base flows because the time required for flow to establish in the separated region is usually significantly greater than the time required for steady flow establishment elsewhere in the flowfield.

The limited flow time available for shock tunnel testing makes it essential for any study which aspires to describe the flow in the separated region to ensure that the flow within that region has reached a steady state. The purpose of this paper is to examine the establishment process of the separated base flow behind a cone at a low- enthalpy hypersonic condition and determine whether the chosen shock tunnel and model configuration can generate a sufficiently long test time to faithfully simulate such flows.

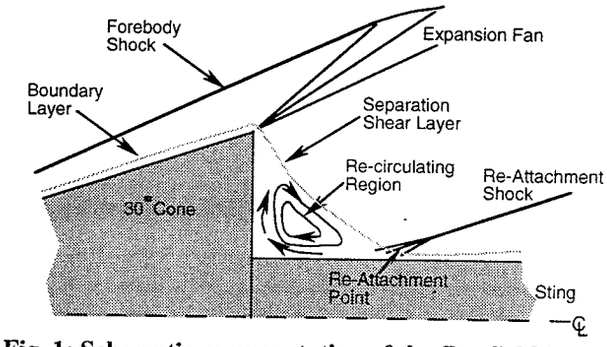

Fig. 1: Schematic representation of the flowfield in the near wake of a cone in hypersonic flow.

Figure 1 shows the main flow features found in a hypersonic near-wake flowfield around a conical body. The near wake is characterised by a region of interaction between the inviscid flow which expands around the shoulder of the cone and a region of low-density, low-velocity viscous flow in the re-circulation region near the base of the body. These two regions interact with each other via the separated boundary layer which lies between them. The presence of the sting generates a re-attachment shock which causes the external flow to be deflected parallel to the sting and the flow within the re-circulating region to be deflected towards the base of the cone. At the reattachment point, the flow is nearly at stagnation conditions and, at high freestream velocities, significant heat transfer occurs.

In these experiments particular attention is paid to the region between the shoulder of the cone, where separation occurs, and the point where the boundary layer re-attaches to the sting. In particular, it is important in the visualisation of the separated region to see the point of re-attachment and the edge of the boundary layer, to provide an indication of the size of the separated region.

1.1 Criteria for Steady Flow Establishment

As described in Tanner's[2] summary paper, supersonic base flows are essentially non-oscillatory, in that the scale of turbulent structures generated by separation are small compared to the size of the base region. Thus, the separated region takes the form of a standing eddy rather than the vortex streets which often occur in subsonic flows.

Holden[3] has investigated the establishment times for separated flow at the base of a sphere in a supersonic flowfield, using a shock tunnel with a relatively long test duration of 10-30 milliseconds. These tests used skin

Copyright © 1998 by ICAS and AIAA. All rights reserved

Copyright © 1998, by the International Council of the Aeronautical Sciences (ICAS)
and the American Institute of Aeronautics and Astronautics, Inc.

friction, surface pressure and heat transfer measurements at the base of the sphere to indicate establishment time in the separated region.

Assuming that the boundary layer on the cone surface has formed, the initial establishment mechanism is associated with the propagation of an acoustic disturbance from the re-attachment point to the separation point. The separated flow then interacts with the surrounding inviscid flow until the conservation equations are satisfied. According to the experiments conducted by Holden, these mechanisms take similar time periods to reach completion. Mallinson *et al.*[4] have used such a technique to estimate establishment time of the separated flow at a compression corner. Following this method, the time taken to establish a steady boundary layer on the cone can be approximated by the empirically-determined boundary layer establishment time for a flat plate

$$\Delta t_{bl} = \frac{3.33x}{U_c} \quad ..1$$

where x is the length from the cone tip to the shoulder and U_C is the velocity of the flow in the cone shock layer. The time for propagation of the acoustic disturbance depends on the sound speed in the boundary layer. As there are temperature gradients in the boundary layer, the temperature is approximated by the reference temperature described by Eckert[5] as

$$T^* = 0.5(T_w + T_c) + 0.11 \cdot \mathrm{Pr}^{1/2}(\gamma - 1)M_c^{\,2}T_c \quad ..2$$

where T_c and M_c are the temperature and Mach number in the cone shock layer, T_w is the wall temperature, Pr is the Prandtl number and γ is the ratio of specific heats. Having determined the average temperature in the boundary layer, the average sound speed, a_δ can be found using

$$a_\delta = \sqrt{\gamma R T^*} \quad ..3$$

The propagation time is then simply described by

$$\Delta t_{sep} = \frac{l_{sep}}{a_\delta} \quad ..4$$

where l_{sep} is the distance between the cone shoulder and the re-attachment point. Thus, knowing the length of the separation region and the flow properties at the shoulder of the cone allows the establishment time to be estimated as $\Delta t_{bl} + 2\Delta t_{sep}$ after the freestream establishment time. This analysis was used to make initial choices of cone step-height, based upon an initial numerical calculation of the size of the separated flow region.

2. Experiment

2.1 Shock Tunnel and Flow Conditions

The experiments were performed using the T2 Free-piston shock tunnel facility at the Australian National University. This facility is described in detail by Stalker[6]. For the experiments described herein, the primary diaphragm had a burst pressure of 46.9 MPa. A 7.5° half-angle conical nozzle with a throat diameter of 6.35 mm and a nozzle-exit diameter of 73.6 mm was used to generate the desired freestream conditions. Pressure transducers located at the nozzle reservoir and another point in the shock tube allow the shock speed and nozzle-reservoir pressure to be measured. These values, along with the fill conditions, are used by the equilibrium shock tube calculation code ESTC[7] to calculate the flow conditions in the nozzle reservoir after shock reflection. These values were then used as an input to the quasi one-dimensional nonequilibrium nozzle flow code STUBE[8], which calculated the freestream flow properties.

Nozzle Reservoir Conditions[9]	
P_0(MPa)	27.9 ± 0.7
T_0(K)	4535 ± 50
ρ_0(kg/m^3)	22.3 ± 0.5
H_0(MJ/kg)	5.29 ± 0.08
Nozzle Exit Conditions[9]	
P_∞(kPa)	4.5± 0.2
T_∞(K)	438 ± 10
ρ_∞(kg/m^3)	0.035 ± 0.001
M_∞ (frozen)	7.63± 0.1
Cone Surface Conditions (Inviscid)	
P_C(kPa)	102
T_C(K)	1640
ρ_C(kg/m^3)	0.16
M_C	3.36
u_C(m/s)	3000
β_C (°)	34.6
Re_C	4.7x10^5

Table 1: Summary of flow properties in the shock tunnel nozzle reservoir, freestream and cone shock layer. Nozzle Reservoir and freestream conditions, with associated uncertainties from Palma (1998).

Flow properties at the cone surface (outside the boundary layer) were obtained from the tabular data of Sims[10] for supersonic perfect gas flows around cones at zero incidence. These data were used to calculate shock angle and Reynolds number at the shoulder of the cone. The nozzle reservoir, freestream and cone surface flow properties are summarised in Table 1. The freestream conditions in Table 1 were chosen because that condition

Copyright © 1998, by the International Council of the Aeronautical Sciences (ICAS)
and the American Institute of Aeronautics and Astronautics, Inc.

had been characterised previously by Palma[9] and the calculated freestream temperature and pitot pressure had been experimentally tested.

The test gas used in the experiments was a mixture of 99% nitrogen and 1% oxygen. Because the test gas is held for several hundred microseconds at the stagnation temperature in the nozzle reservoir, the molecular oxygen and some of the molecular nitrogen dissociate and form NO (nitric oxide) which is used as the absorbing species for the PLIF visualisation. The 1% mole fraction was chosen as a compromise between maximising PLIF signal strength and minimising laser beam attenuation.

The test time used for previous experiments performed using this flow condition was 350 μs after shock reflection. After the initial pressure increase associated with the reflection of the primary shock at the shock tube end wall, the nozzle-reservoir pressure stays roughly constant for approximately 300 μs, after which the pressure decreases at a rate of about 2 MPa per 100 μs. The present series of experiments examined the flow properties at 54, 68, 80, 100, 150, 200, 250, 300, 350 and 400 μs after shock reflection. These tests span the entire test time at this condition and also include the nozzle flow starting processes.

The model used was a stainless steel cone with a half-angle of 30° and a base diameter of 50 mm. The sting was 80-mm long and 25.5 mm in diameter. The height of the base region was 12.5 mm. The sting and base of the model were painted black to minimise the effect of laser scatter from the model surface.

2.2 PLIF System

Planar laser-induced fluorescence (PLIF) is a technique which has proved useful for both visualisation and quantitative flowfield measurements in a variety of supersonic and hypersonic flows[11,12]. PLIF involves the use of a sheet of laser light tuned to excite an electronic transition in an atomic or molecular species. The molecule fluoresces and the fluorescence is then captured, typically using an intensified CCD camera. The intensity of the fluorescence depends upon the temperature of the flow and the number density of molecules in the state excited by the laser. Flow features which cause changes in these quantities, such as shock waves, expansion waves and mixing regions, can be visualised using the differing signal intensities in these regions.

The experimental arrangement of the PLIF visualisation system is shown in Fig. 2. Laser radiation at a wavelength of 308 nm provided by a XeCl excimer laser (Lambda Physik EMG150ETS) was used to pump a tunable dye laser (Lambda Physik Scanmate II), operating at wavelengths near 450 nm. The output of the dye laser was then frequency doubled using a BBO-I doubling crystal. A combination of a 30-mm focal length cylindrical lens and a 1000-mm focal length spherical lens was used to form the doubled light into a sheet. The sheet was approximately 60-mm wide and approximately 0.8-mm thick. The energy of the doubled dye laser output was approximately 4 mJ, with a Gaussian spectral width of 0.18 cm^{-1} and a pulse length of 25 ns.

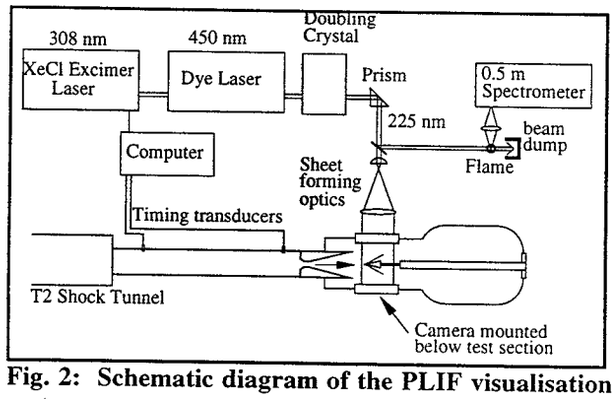

Fig. 2: Schematic diagram of the PLIF visualisation system.

A small portion of the beam was diverted before reaching the sheet-forming optics and passed through a hydrogen/oxygen flame. The fluorescence induced in the flame was measured using a 0.5-m spectrometer. A fluorescence excitation scan was performed just prior to each shock tunnel test to ensure that the laser was tuned to the peak of the absorption line being probed.

The PLIF system was triggered (after a pre-set delay time) by the pressure pulse measured by the arrival of the shock at the nozzle reservoir pressure transducer. After a second pre-set delay, which accounted for the time between the laser trigger pulse and the firing of the laser, a Princeton Instruments intensified CCD camera (576 by 384 pixels, 16-bit dynamic range, 50 ns minimum gating time) was triggered and the fluorescence recorded. The gate time of the intensifier was 80 ns. A Schott glass UG-5 filter was placed in front of the camera to filter out laser scatter whilst allowing the non-resonant fluorescence to pass into the camera.

Images were corrected for the spatial energy profile of the laser sheet by normalising to PLIF images obtained in a quiescent mixture of 1% NO in N_2 prior to the experiments. A photodiode was used to monitor pulse-to-pulse variations in laser energy.

3. Results and Discussion

3.1 Line Selection

The flow within the separated region has a higher temperature and much lower pressure and velocity than the surrounding inviscid flow. This wide variation of flowfield properties makes the base flow around a cone in a hypersonic freestream a challenging flow to image. Previous experiments using Mie scattering to visualise the near wake around a boat-tailed afterbody were unable to visualise the re-circulation region because high temperatures would cause the ethanol to evaporate[13]. Also, probe-based measurement techniques have been shown to significantly interfere with the structure of the flow in the re-circulation region[14]. Therefore any visualisation or measurement technique must be capable

Copyright © 1998, by the International Council of the Aeronautical Sciences (ICAS)
and the American Institute of Aeronautics and Astronautics, Inc.

of detecting very small number densities to provide adequate measurement sensitivity.

Initial tests were performed to determine which transition was most suitable for the purpose of visualising the flow around the cone. Criteria for suitability were isolation of the transition, overall LIF signal strength and sufficient difference in LIF signal strength to allow clear differentiation of the different regions of the flow, in particular the re-circulation zone and the re-attachment shock.

Isolated transitions having three different values for rotational quantum number (J'') were chosen. Higher J'' values tend to provide relatively high signal at high temperatures and lower signal levels at low temperatures, the opposite trend prevailing for low J'' values. This is because high J'' states are more populated at higher temperatures[15]. The three transitions initially used for visualisation were ${}^{O}P_{12}$ (J''=2.5) at 44068.9 cm^{-1}, ${}^{S}R_{21}$ (J''=17.5) at 44411.3 cm^{-1} and Q_1 + ${}^{Q}Q_{11}$ (J''=28.5) at 44404.6 cm^{-1} in the $A^2\Sigma^+ \leftarrow X^2\Pi(0,0)$ absorption band of nitric oxide (NO). Images obtained using these transitions showed that the best differentiation between different regions of the flowfield was obtained using the ${}^{S}R_{21}$ (J"=17.5) transition. This transition was used for all results presented in this paper.

3.2 Repeatability of Visualisation Results

Four tests were performed at the 350 μs test time, to determine the degree of shot-to-shot variation in the flow conditions. Fig. 3 is an average of these images. It clearly shows the position of the forebody shock wave and the expansion around the shoulder of the cone. The cone itself occupies the lower left section of the picture and the sting occupies the lower part of the image. The separated shear layer between the re-circulating and inviscid flows is clearly visible, as is the re-attachment point, located 1.7 base heights from the base of the cone. The re-attachment shock and post-shock flow can be seen as a bright region just downstream of the re-attachment point.

The nozzle boundary layer and the extent of the core flow is also shown in Fig. 3, as the slightly darker region at the top left of the image. The presence of the nozzle boundary layer causes the forebody shock and shoulder expansion to be refracted towards the top of the picture. The bright patches on the surface of the cone and the sting are due to laser scatter from the surface of the model.

It is apparent from Fig. 3 that several of the flow features are stable enough to indicate good shot-to-shot repeatability in the flow. The positions of the forebody shock, re-attachment shock and shoulder expansion fan are clearly delineated. There is some variability in the shape of the re-circulation region itself, indicated by the slightly blurred outline of the region in Fig. 3. The averaging of the images indicates that at the optimum test time, the inviscid part of the flow had fully stabilised, but the viscous re-circulation zone had not. This finding was supported by the images of the time-evolution of the flowfield presented in the next section. The average of the four images, as would be expected, provide a much clearer picture of the re-circulation region than the single-shot images in Fig. 4.

Fig. 3: Average of four images acquired at t=350 μs after shock reflection. Flow is from left to right and the cone tip is out of the field of view, to the left of the image.

3.3 Time Evolution of Flow

Figure 4 is a collection of single images obtained at several delay times, showing the development of the base flow during the test time. One major difficulty encountered when obtaining these images was the large range of signal intensities in different parts of the flow. The images obtained between 250 and 400 μs after shock reflection filled the entire dynamic range of the camera. The expansion region registered nearly 60 000 counts, while the re-circulation zone only registered around 500 counts above background. This made viewing both regions in the one image difficult. For this reason, the natural logarithm was taken of the images from the CCD camera and the result multiplied by 16 to give the images shown in Fig. 4 as 8-bit greyscale images. This had the effect of accentuating changes in the lower part of the camera's range and reducing them in the upper part of the range, allowing all signal levels to be visualised in the one image.

The 54 μs image shows the starting shock from the nozzle as it passed over the cone. The signal in this image is higher than might be expected, which may be due to Mie scattering from detritus in the shock tube, carried by the starting shock. Although the UG-5 filter was supposed to remove the scatter from these sources, some laser light must still have been transmitted. The dark strip at the left of each of the images in Fig. 4 indicates a region of the flowfield not illuminated by the laser sheet. The low signal level in this region indicates that the signal contribution from flow luminosity is small.

Experiments visualising flow in the near wake of a circular cylinder, performed by Liang *et al.* [15] show a similar curved starting shock moving past the base of their model. The schlieren system also visualised fine

Copyright © 1998, by the International Council of the Aeronautical Sciences (ICAS)
and the American Institute of Aeronautics and Astronautics, Inc.

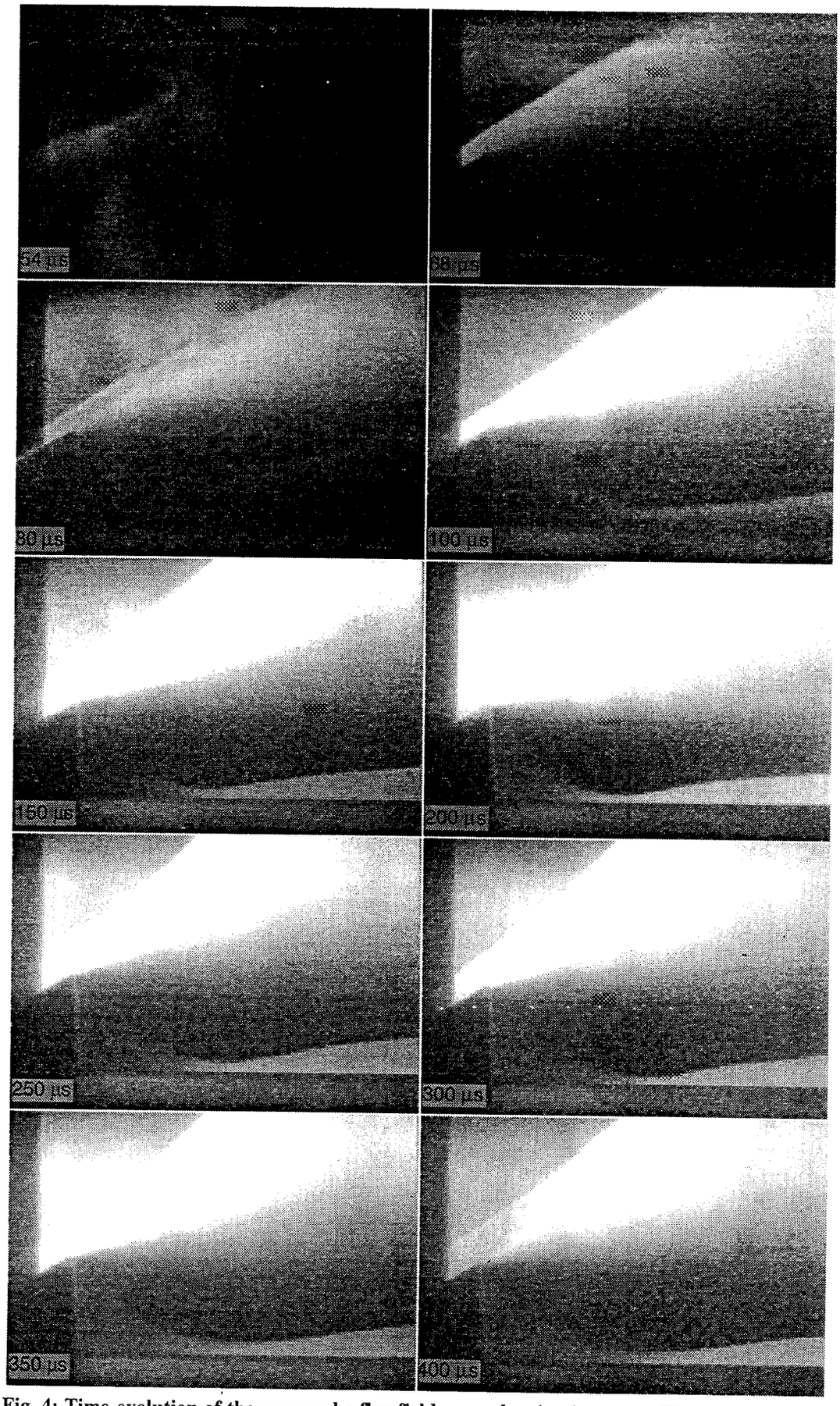

Fig. 4: Time-evolution of the near-wake flowfield around a circular cone. Times are relative to shock reflection.

Copyright © 1998, by the International Council of the Aeronautical Sciences (ICAS)
and the American Institute of Aeronautics and Astronautics, Inc.

structure in the establishing base flow which is not apparent in Fig. 4, presumably because the temperature variations in this region are not large enough to make these structures apparent using PLIF visualisation.

At 68 and 80 μs the forebody shock and expansion have started forming, but no signal occurs in the re-circulation region, which can only be seen from 100 μs after shock reflection. The freestream signal appears to have stabilised by 100 μs.

The shock layer and expansion stabilise by 150 μs after shock reflection, but the images from 150 to 400 μs show significant fluctuations in the size of the re-circulation zone, the height of the 'neck' at the re-attachment point and the shape of the re-attachment shock behind the base of the cone.

In order to quantify the establishment process, three important values were measured in each of the images: the height of the shock above the shoulder of the cone, the height of the 'neck' at the re-attachment point and the distance of the re-attachment point from the base of the cone. These quantities are plotted in Fig. 5.

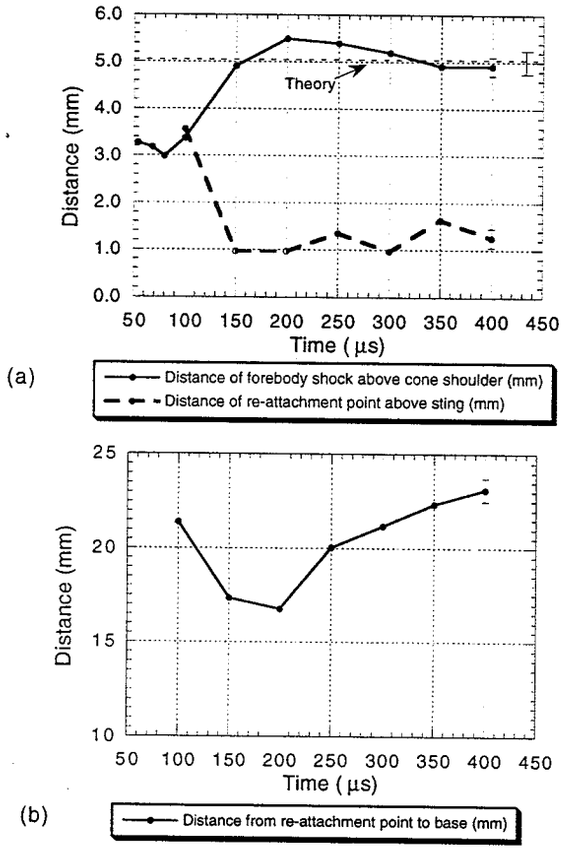

Fig. 5: Time-evolution of measured quantities from images in Fig. 4. (a) Variation of shock position above cone shoulder and height of re-compression neck above sting. (b) Variation of distance from rearward stagnation point to cone base.

Fig. 5(a) shows the variation of forebody shock height and re-compression 'neck' height throughout the flow time. The forebody shock position is seen to stabilise at 300-350 μs to a value of around 5.0 mm above the shoulder of the cone. The dashed line indicates the expected position of the shock assuming the freestream conditions calculated using ESTC and STUBE. The uncertainty in this calculated value represents the difference between frozen and equilibrium solutions. The two values agree reasonably well, indicating that the shock and the flow in the shock layer has completely established by around 300 μs after shock reflection.

The lower plot in Fig. 5(a) indicates that the flow in the near wake of the cone may not have stabilised. There appears to be some oscillation in the width of the 'neck' at the re-attachment point which still occurs at the 400 μs delay time. This suspicion is reinforced by the plot in Fig. 5(b) of the distance of the re-attachment point from the base of the cone. There is clear evidence that the size of the re-circulation region is increasing even at the 400 μs delay time. The gradual increase in the distance of the re-attachment point to the cone base indicates that the re-circulation region is filling throughout the constant pressure test time and does not reach a stable equilibrium.

If the maximum displacement of the re-attachment shock from the base of the cone is used as a measure of the size of the re-circulation region, the distance from this point to the shoulder of the cone can be used in the calculation of estimated establishment time discussed in Section 1.1. Evaluating equations 1 through 4, using the calculated cone surface flow conditions results in a boundary layer establishment time of $\Delta t_{bl} = 46$ μs and a sonic propagation time of $\Delta t_{sep} = 23$ μs. The measured beginning of steady flow in the nozzle is about 100 μs after shock reflection. Combining these values and making the assumption that the time for the viscous-inviscid interaction between the re-circulation and expansion flows is approximately the same as Δt_{sep} gives a calculated establishment time of approximately 190 μs. It would seem from the visualisations that this is an underestimate of the establishment time. The most likely error in the calculation lies in the assumption that the two processes involved in establishing the re-circulating flow take a similar amount of time to complete[3]. The images indicate that the interaction between the flow in the re-circulation region and the surrounding flow takes considerably longer to equilibriate in a base flow than the time for sonic information to traverse the re-circulation zone.

The establishment time calculated above corresponds to the pressure stabilisation time measured by Holden [3] for wake flows on spheres. Those experiments found, however, that the time required for heat transfer to reach equilibrium was more than twice as long as the pressure establishment time and can be described by the equation

$$\Delta t_{sep} = \frac{70 \cdot D}{U_c} \qquad ..5$$

Copyright © 1998, by the International Council of the Aeronautical Sciences (ICAS)
and the American Institute of Aeronautics and Astronautics, Inc.

where D is the base diameter of the cone and U_C is the inviscid flow velocity at the cone surface just upstream of the separated region. Substituting our flow conditions into this empirical relation generates an establishment time of 560 μs. Our results indicate that the establishment time is better described by Holden's heat transfer establishment time than the pressure establishment time.

4. Conclusions

These experiments have shown that PLIF is a viable technique for qualitative visualisation of the time-evolution of the base flow around a cone of 30° half-angle in a hypersonic flow. The technique allowed all of the basic flow regions in the freestream, shock layer and near wake to be seen.

Measurements taken from the images in Fig. 4 indicated that the flow in the near wake had not completely stabilised by the end of the steady flow time of the T2 shock tunnel.

Comparison of our measurements with the analysis of section 1.1 indicate that the calculation underestimates the time required to achieve steady flow in the re-circulating region. This is possibly because the interaction between the re-circulating flow and the surrounding inviscid flow takes significantly longer to stabilise than the time taken for information about the surrounding flow to traverse the re-circulating region. This result is consistent with the heat transfer measurements of Holden[3].

Future Work

Future tests will be performed with smaller base heights, to generate a separated base flow which has sufficient time to establish during the available test time. Using equation 5 as a guide, a step height of 6 mm would allow the base flow to establish by approximately 300 μs after shock reflection.

The low density and high temperature in the re-circulation zone made it difficult to achieve large signal levels (or significant variations in signal) in that region. For this reason, the structures and variations in flow properties within the re-circulating region were not apparent, although the interface between the re-circulation zone and the surrounding flow could be seen more clearly using an average of four images.

There are two main improvements which could lead to greater signal in the re-circulation zone. A cylindrical lens with a longer focal length could be used to make a narrower laser sheet with a higher energy density. An even more significant improvement in signal could be obtained by using a significantly longer gate time on the camera intensifier. The 80 ns gate time was much shorter than the fluorescence lifetime of 115 ns in the re-circulation region, but of the same order as the lifetime of the fluorescence in the shock layer. Thus using a longer gate time would increase the signal from the re-circulation zone significantly without increasing the signal from the shock layer or expansion region. The ability to vary the delay between the firing of the laser and acquisition of the PLIF image can also be used to vary the relative size of the signals in different parts of the flowfield, allowing higher gains to be used for measurements in the separated region without saturating the flow in the shock layer. Future tests will be performed to explore these possibilities and improve the sensitivity in this critically important part of the flowfield.

PLIF thermometry measurements using the two-line technique outlined in Eckbreth[15] are also planned. This will allow the time-development of the temperature distribution in the near wake of the cone to be measured, which may provide a clearer indication of when separated flow is completely established.

Acknowledgments

The authors willingly express their gratitude to Mr. M. Gaston for initial CFD modelling of the flow properties around the base of the cone, upon which NO absorption lines were selected. This series of experiments was funded by the Australian Research Council.

References

1. Gai, S.L. (1992), Free piston shock tunnels: developments and capabilities. Prog. Aerospace Sci. 29:1-41.

2. Tanner, M. (1984), Steady base flows. Prog. Aerospace Sci. 21: 81-157.

3. Holden, M.S. (1971), Establishment time of laminar separated flows. AIAA Journal, 9:2296-2298.

4. Mallinson, S.G., Gai, S.L. and Mudford, N.R. (1997), Establishment of steady separated flow over a compression-corner in a free-piston shock tunnel, Shock Waves, 7:249-253.

5. Eckert, E.R.G. (1955), Engineering relations for friction and heat transfer to surfaces in high velocity flow, J. Aeronautical Sci., 22:585-587.

6. Stalker, R.J. (1967), A study of the free-piston shock tunnel, AIAA Journal, 5:2160-2165.

7. McIntosh, M.K. (1968), Computer program for the numerical calculation of frozen equilibrium conditions in shock tunnels. Internal report, Department of Physics, The Faculties, Australian National University.

8. Vardavas, I.M. (1984), Modelling reactive gas flows within shock tunnels. Australian J. Phys, 37:157-177.

9. Palma, P.C. (1998), Laser-induced fluorescence imaging in free-piston shock tunnels. Ph.D. thesis, Australian National University.

Copyright © 1998, by the International Council of the Aeronautical Sciences (ICAS)
and the American Institute of Aeronautics and Astronautics, Inc.

10. Sims, J.L. (1964), Tables for supersonic flow around right circular cones at zero angle of attack. NASA SP-3004.

11. Palmer, J.L. and Hanson, R.K. (1994), Shock tunnel flow visualization using planar laser-induced fluorescence imaging of NO and OH. Shock Waves 4:313-323.

12. Palma, P.C., McIntyre, T.J. and Houwing, A.F.P. (in press), PLIF thermometry in shock tunnel flows using a Raman-shifted tunable excimer laser. To be published in Shock Waves

13. Dutton, J.C., Herrin, J.L., Molezzi, M.J., Mathur, T. and Smith, M.K. (1995), Recent progress on high-speed separated base flows.

14. Hawkins, R. and Trevett, E. (1966), Changes in the flow at the base of a bluff body due to a disturbance in its wake, AGARD Report 539.

15. Eckbreth, A.C. (1996), Laser diagnostics for combustion temperature and species. Second Edition, Gordon and Breach, SA, pp. 99-102.

16. Liang, P., Bershader, D. and Wray, A. (1981), Optical studies of shock generated transient supersonic base flows. Shock tubes and Waves, pp. 200-208.